International Journal of Nanomedicine

Dovepress
open access to scientific and medical research

Open Access Full Text Article

ORIGINAL RESEARCH

Development of decellularized meniscus using closed sonication treatment system: potential scaffolds for orthopedics tissue engineering applications

This article was published in the following Dove Press journal:
International Journal of Nanomedicine

Fatihah Yusof[1]
Munirah Sha'ban[2]
Azran Azhim[1]

[1]Department of Biomedical Sciences, Kulliyyah of Allied Health Sciences, International Islamic University Malaysia, Kuantan, Malaysia; [2]Department of Physical Rehabilitation Sciences, Kulliyyah of Allied Health Sciences, International Islamic University Malaysia, Kuantan, Malaysia

Purpose: Meniscus is a fibrocartilagenous tissue that cannot effectively heal due to its complex structure and presence of avascular zone. Thus, tissue engineering and regenerative medicine offer an alternative for the regeneration of meniscus tissues using bioscaffolds as a replacement for the damaged one. The aim of this study was to prepare an ideal meniscus bioscaffold with minimal adverse effect on extracellular matrix components (ECMs) using a sonication treatment system.

Methods: The decellularization was achieved using a developed closed sonication treatment system for 10 hrs, and continued with a washing process for 5 days. For the control, a simple immersion treatment was set as a benchmark to compare the decellularization efficiency. Histological and biochemical assays were conducted to investigate the cell removal and retention of the vital extracellular matrix. Surface ultrastructure of the prepared scaffolds was evaluated using scanning electron microscope at 5,000× magnification viewed from cross and longitudinal sections. In addition, the biomechanical properties were investigated through ball indentation testing to study the stiffness, residual forces and compression characteristics. Statistical significance between the samples was determined with p-value =0.05.

Results: Histological and biochemical assays confirmed the elimination of antigenic cellular components with the retention of the vital extracellular matrix within the sonicated scaffolds. However, there was a significant removal of sulfated glycosaminoglycans. The surface histoarchitecture portrayed the preserved collagen fibril orientation and arrangement. However, there were minor disruptions on the structure, with few empty micropores formed which represented cell lacunae. The biomechanical properties of bioscaffolds showed the retention of viscoelastic behavior of the scaffolds which mimic native tissues. After immersion treatment, those scaffolds had poor results compared to the sonicated scaffolds due to the inefficiency of the treatment.

Conclusion: In conclusion, this study reported that the closed sonication treatment system had high capabilities to prepare ideal bioscaffolds with excellent removal of cellular components, and retained extracellular matrix and biomechanical properties.

Keywords: sonication, meniscus, scaffolds, decellularization, tissue engineering, regenerative medicine

Correspondence: Azran Azhim
Department of Biomedical Sciences, Kulliyyah of Allied Health Sciences, International Islamic University Malaysia, 25200 Bandar Indera Mahkota, Kuantan, Malaysia
Tel/Fax +60 9 570 5265
Email azranazhim@iium.edu.my

Introduction

Meniscus is a triangular crescent-shaped wedge of fibrocartilage comprised of medial and lateral component that is located between the tibial plateau and femoral condyles of the knee.[1] This kind of tissue plays important roles in the knee including

submit your manuscript | www.dovepress.com
DovePress
http://doi.org/10.2147/IJN.S207270

distributing stress evenly, protecting the cartilage, lubricating knee joints and also being used as a shock absorber.[2] There are two types of meniscal injury that cause discomfort for a significant number of patients, known as acute and degenerative tears. Acute tears generally relate to sports activities, while degenerative tears are an age-related disease that commonly occurred in middle-aged to older adults.[3] Meniscus injury that occurred within the tissues can be classified based on tear pattern, location and thickness.[4] Different types of tear patterns exist comprised of vertical/longitudinal, flat/oblique, radial and horizontal tear. Tears might locate within the peripheral vascularized zone (red zone), middle area (red-white zone) or inner avascular portion (white zone). Lack of vascularization especially within the area of white-red and white zone causes low regenerative properties and low healing capability at the injury site.[5]

The principal methods for the surgical management of meniscal injury are classified into meniscectomy, meniscal repair and meniscal reconstruction. Each method has its pros and cons in long-term result. Meniscectomy involves the removal of the torn meniscus either totally or partially which consequently can develop into early osteoarthritis.[6,7] For meniscal repair, the surgeons will repair the torn in the meniscus if it is reasonable under arthroscopy. Latest therapeutic approach is meniscus reconstruction using either allograft transplant or meniscus scaffolds that aim to replace the resected meniscus with a functional meniscus that structurally mimics the native meniscus.[7,8] However, this allograft transplantation was reported to cause a possible complication of immune rejection by the recipient and there is a chance of introducing infection or disease that leads to failure of the transplant.[9]

The emerging tissue engineering concept is used to regenerate new tissues using natural or synthetic scaffolds. Natural scaffolds known as bioscaffolds are increasingly being utilized nowadays. The bioscaffolds need to undergo decellularization process to remove the cells and DNA while preserving the structure of the tissues to prepare minimally immunogenic scaffolds.[10] There are three categories of decellularization techniques known as chemical, enzymatic and physical that might give a different effect on the scaffolds based on antigenic removal efficiency, tissues structure composition and mechanical strength. The choice of decellularization method varies depending on the characteristics of the particular tissues itself such as geometric considerations, cells and matrix density, and it is encouraged that this method be applied in combination.[11,12]

Sonication treatment system is one of the promising physical decellularization techniques where this system applies an ultrasound sonication in SDS solution. Previously, it was reported that the open sonication system successfully prepared aorta scaffolds with complete cell removal and managed to preserve the structure of the tissues and extracellular matrix component (ECM) components.[13–16] For meniscus tissue decellularization using this system, a primary study was done using 20 kHz frequency with 2% SDS solution for 10-hr treatment time that resulted in highest cell removal, but there was a minor presence of cells observed.[17] Thus, further study is required by increasing the frequency to 40 kHz while minimizing the SDS concentration to 0.1% in order to preserve the bioscaffold properties.

In 2017, Azhim et al developed a closed sonication system as an improvement of the functionality from the previous open system. This newly developed closed system consists of two compartments; incubator and chiller as portrayed in Figure 1. The incubator consists of an ultrasonic transducer, hydrophone, multiparameter probe, temperature monitor, water bath and sample holder. This development aims to improve the hygiene and sterility of the system to prevent any bacterial contamination and to maintain the temperature of the solution throughout the treatment. In this current study, the developed closed sonication treatment system was utilized for decellularization process.

The purpose of this study is to prepare and evaluate the decellularized scaffolds using developed closed sonication treatment system that includes 40 kHz frequency in 0.1% SDS solution. The characterizations of the scaffolds were evaluated using various analyses. Histological analyses were completed to detect cellular component removal and ECM components distribution. Scanning electron microscopy was utilized to observe the surface ultrastructure. The biochemical assays and biomechanical properties were conducted as well to investigate the changes in DNA, collagen, glycosaminoglycan (GAG) content and also the scaffold strength.

Materials and methods

Preparation of tissue samples

The fresh samples of the meniscus derived from bovine were purchased from the local slaughterhouse situated at Kuantan. The samples were kept in 1x PBS (4°C) once collected and stored in −20 until further usage. The samples were thawed and sliced into the desired size (10 mm×10 mm×3 mm) for decellularization process.

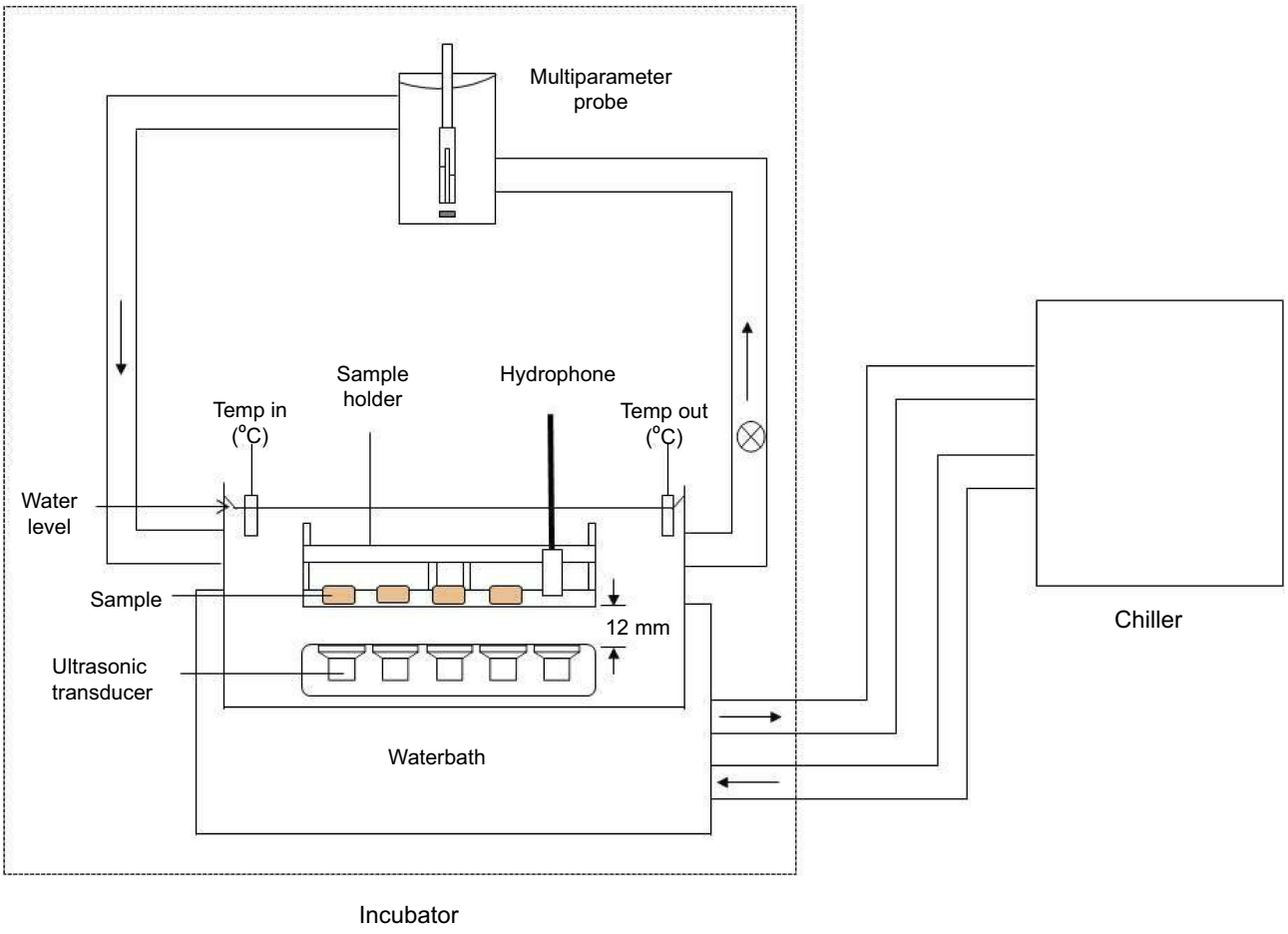

Figure 1 Developed closed sonication treatment system that consists of incubator and chiller compartments.
Abbreviation: Temp, temperature.

Decellularization process

For decellularization process, two types of treatments were completed that comprised of simple immersion and sonication treatment to investigate the effectiveness of 40 kHz sonication frequency for decellularization. The process was carried out as described below.

Sonication decellularization treatment

For sonication decellularization, the process was conducted in a closed sonication treatment system that involved the use of ultrasonic power. The position of the samples was fixed at 12 mm above the transducer. The frequency and temperature of 0.1% SDS solution was set at 40 kHz and 36±1 °C, respectively, with a treatment time of 10 hrs.

Immersion decellularization treatment

An immersion decellularization treatment was set as control that had similar parameters: temperature, SDS concentration and treatment time with the exception of ultrasound frequency. There was an assistance of 70 rpm agitation for immersion treatment in order to create a homogenous condition for decellularization process.

Washing process

The decellularized samples after immersion (n=3) and sonication treatments (n=3) were washed through immersion in 1x PBS with constant shaking for 5 days. The PBS solution was changed every 24 hrs. For the evaluation process, there were three groups compared that comprised of native, immersed and sonicated scaffolds.

Histological analyses for cell removal and ECM preservation

Native (n=3) and decellularized tissue samples (n=3) were fixed in neutral buffered saline (NBF) with the respective conditions (24 hrs, 4°C), embedded in paraffin block (EG1160, Leica Biosystems, Buffalo Grove, IL, USA) and the samples were frozen on a cold plate. The paraffin-

embedded tissues were sectioned using manual rotary microtome (RM 2235, Leica Biosystems, Illinios, USA) to obtain 8 μm ribbons and stained using H&E, safranin O/fast green and picro-sirius red staining. Hematoxylin & eosin staining was conducted to evaluate the cell removal while safranin O/fast green and picro-sirius red staining to visualize the GAG and collagen network distribution.

Biochemical assays

Prior to DNA quantification, the native (n=3) and decellularized samples (n=3) were weighed and incubated overnight in Proteinase K solution with lysis buffer solution (Bioneer, Daejeon, Korea). AccuPrep Genomic DNA Extraction Kit from Bioneer (Korea) with the standard protocol provided by the manufacturer to purify the DNA from each sample was utilized. The purity and yield of the nucleic acid obtained will be quantified by using the spectrophotometer at 260 nm and 280 nm optical density. By referring to the 260/280 ratio result, the data ranges from 1.8 to 2.0 will be collected and evaluated.

For collagen content, it was quantified using Sircol Collagen assay kit from Biocolor Ltd (Newtownabbey, UK) following manufacturer recommendations. Briefly, the samples (n=3) were digested in cold acid pepsin comprised of 2.0 mg/mL pepsin in 0.5M acetic acid and incubated at 4 °C overnight. The digested samples were assayed using Sircol dye reagent based on specific binding of sirius red dye to collagen. The absorbance was read at 555 nm using a microplate reader.

The level of GAGs was determined using Blyscan Sulfated Glycosaminoglycan assay kit (Biocolor Ltd, Newtownabbey, UK). The lyophilized samples (n=3) were digested using papain extraction reagent that consisted of 2 mg/mL papain enzyme in 0.2M sodium phosphate buffer and incubated at 65°C overnight. The digested samples were centrifuged, and the pellet obtained was assayed using the 1,9-dimethylene blue dye binding assay (Biocolor Ltd.) following the manufacturer instructions. The mixture was incubated for approximately 30 mins and centrifuged to ensure the firmly packed GAG–dye complex gathered as a pellet. The GAG–dye complexes were recovered using dissociation reagent, and the contents were measured using microplate reader at 656 nm.

Surface ultrastructure evaluation

The tissue samples (n=3) were fixed in 4% McDowell–Trump solution at 4°C for 24 hrs. The scaffolds were washed with a buffer solution (0.2 M phosphate buffer) and post-fixed in 0.1% osmium tetroxide for 1–2 hrs at room temperature. The process continued with washing process using phosphate buffer followed by graded alcohol gradient (50% to 100%) and drying process in critical point drying (CPD). Samples were subjected to mounting equipment for gold (Au) sputter coating for 60 s. The samples were viewed by using scanning electron microscope (Carl Zeiss, Germany) with 5,000x magnification.

Biomechanical characterization

The native (n=3) and decellularized meniscus samples (n=3) were trimmed into a square shape (6 mm×6 mm) with a thickness of 3 mm. It was placed horizontally in a customized designed metallic plate to prevent the dislocation of the samples under the indentation testing device. A universal testing machine MX-500N (IMADA, Japan) accompanied with digital force analyzer FA PLUS (IMADA, Toyohashi, Japan) was utilized to perform compression–relaxation test.

A repetitive ball indentation testing was performed using 3 mm steel ball indenter. For each cycle, the position of the indenter was calibrated to zero. Throughout the test, the samples were moistened using a physiological saline solution. The indentation test was started with pre-loading on the samples and proceeded with these three phases: 1) dynamic compression of the sample until the peak of the 7N load was achieved with a constant load velocity of 10 mm/min; 2) static compression when the indenter with a constant load of 7N remained in the position for 40 s; 3) relaxation phase is an unload process with a constant velocity of 10 mm/min until 0N was achieved. After 30 s, the described test cycle was repeated for another three times to obtain the load-time (L-T) in Figure 2 and load-displacement (L-D) graph in Figure 3. For each sample, the measurement was performed repeatedly for 3 cycles. A F-S recorder Software was used to display time, load and indenter position where compression, residual force and stiffness would be calculated. The linear elastic slope between 2N and 5N obtained from load–displacement (L-D) graph that is denoted by a red line in Figure 3 represents the stiffness characterization. As for relative compression, it was measured by the indenter position in relation to the absolute sample height.

Statistical analysis

The data were given as mean ± SD. Student *t*-test was used to determine the statistical significance between the different groups. Data were analyzed using SPSS17.0, and $p<0.05$ was considered statistically significant.

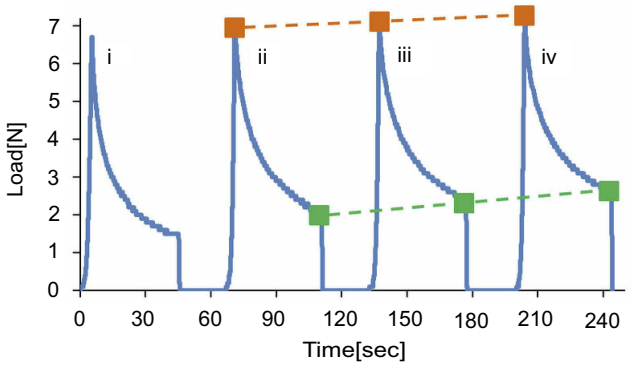

Figure 2 Graph of load (N)] against time (s) comprised of preloading cycle (i), 1st cycle (ii), 2nd cycle (iii) and 3rd cycle (iv). The orange dashed line shows the compression force and the green dashed line shows the residual forces.

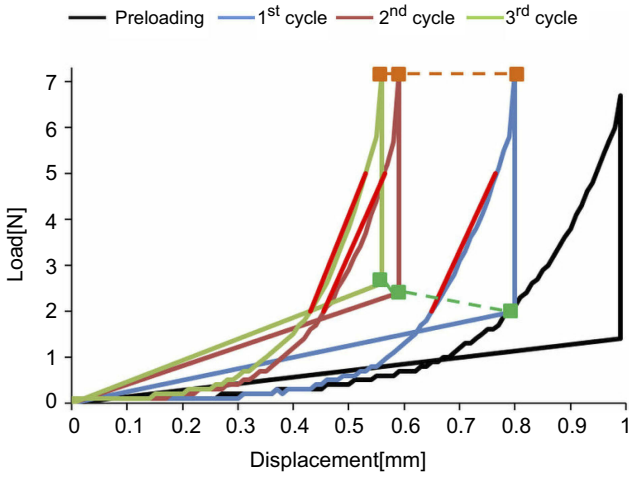

Figure 3 Graph of load [N] against displacement [mm] comprised of preloading cycle, 1st cycle, 2nd cycle and 3rd cycle. Red line slope represents the stiffness of each cycle.

Results

Histological analyses of cell removal

Analysis of the cellsremoval for the sonicated meniscus scaffolds was completed using H&E staining. Based on Figure 4, there was an absence of blue-black nuclei stained in the sonicated meniscus scaffolds compared to immersed scaffolds and native tissues. The nucleus staining (red circle) can be observed in native tissues (i, iv) and immersed scaffolds (ii, v) on the central and surface part of tissues.

Histological analyses of collagen distribution

Picro-sirius red staining was utilized to reveal the collagen distribution within the structure of the tissues as shown in Figure 5. The yellow and green color of collagen bundles represents collagen Type I and Type III, respectively. The immersed scaffolds had more porous structure and lack of type III collagen bundle distribution compared to the preserved and intact collagen bundles represented in sonicated scaffolds that resemble native tissues.

Histological analyses of GAG distribution

Based on safranin O/fast green staining, the red and green stains represented the GAGs and noncollagen contents, respectively, as shown in Figure 6. It can be observed that sonicated and immersed scaffolds had lack of GAG distribution exhibited by red stains. However, the GAGs in sonicated scaffolds were well-preserved and resembled native tissues compared to immersed scaffolds.

Biochemical assays

Based on the DNA quantification assay, there was a significant difference ($p<0.05$) between native tissues, immersed and sonicated scaffolds. The native, immersed and sonicated scaffolds consisted of 28.89±0.936 ng/mg, 9.26±0.254 ng/mg and 2.30±0.071 ng/mg of DNA content.

As for collagen content, native tissues had 613.36 ±5.882 ng/mg, while immersed and sonicated scaffolds had 680.58±7.751 ng/mg and 770.89±7.99 ng/mg, respectively, as shown in Figure 7. Sulfated GAG content of sonicated scaffolds showed a remarkable reduction compared to native where only 39% of the GAGs were retained. The amount of sulfated GAGs reduced from 149.83±13.75 ng/mg to 57.82±3.61 ng/mg with significant difference ($p<0.05$).

Surface ultrastructure observation

The scanning electron microscope with 5,000x magnification showed the orientation and arrangement of the collagen fibrils from the longitudinal and cross-section, respectively. Based on Figure 8, the sonicated and immersed scaffolds showed minor disruption on orientation with loose arrangement of collagen fibrils compared to packed arrangement in native tissue. For cross-section observation, sonicated scaffolds portrayed the presence of micropores.

Biomechanical characterization

The indentation testing was accomplished to investigate the biomechanical characteristics of meniscus scaffolds. The viscoelastic behaviors of the samples comprised of stiffness, compression and residual forces were retrieved from this test. Based on the bar graph shown in Figure 9,

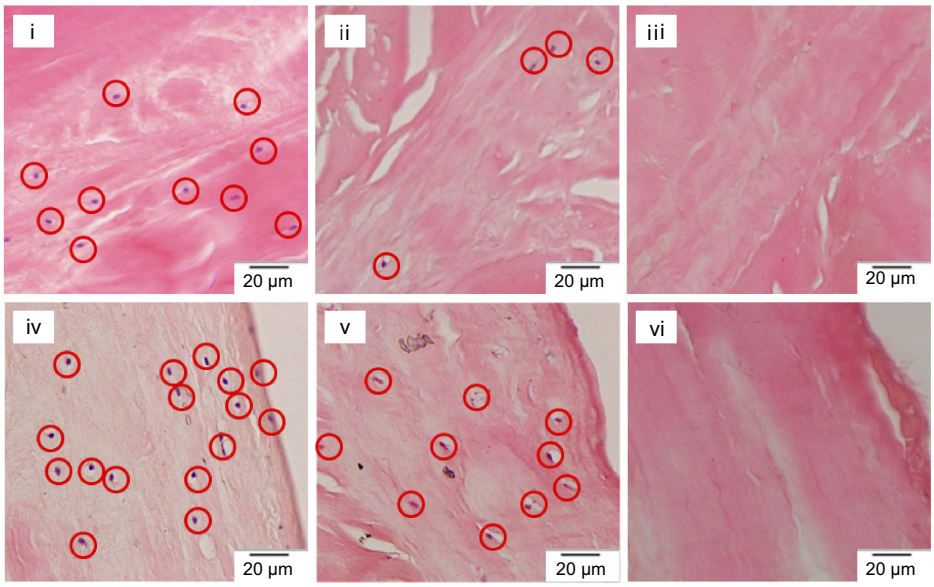

Figure 4 H&E staining of native tissues (i, iv), immersed scaffolds (ii, v) and sonicated scaffolds (iii, vi) from central and surface parts, respectively, with a magnification of 40×. The red circles represent the stained nuclei.

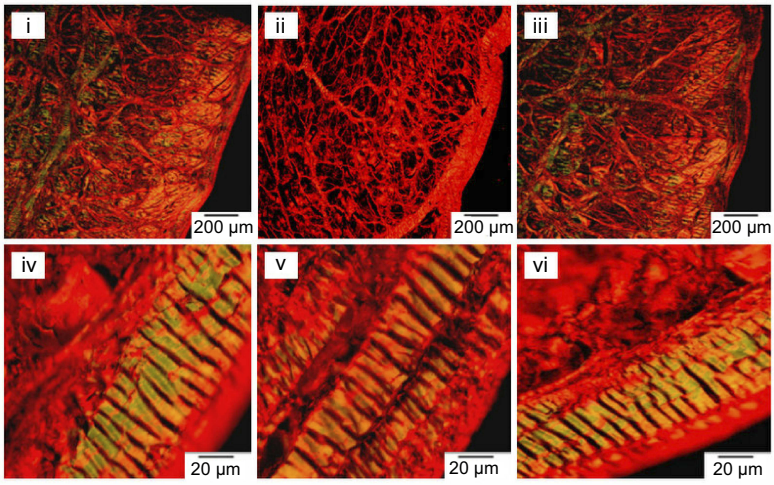

Figure 5 Picro-sirius red staining of native (i, iv), immersed scaffolds (ii, v) and sonicated scaffolds (iii, vi) with a magnification of 4× (i, ii, iii) and 40× (iv,v,vi).

there was gradual increment from cycle 1 to cycle 3 for native, immersed and sonicated scaffolds for all biomechanical properties. For example, compression data from cycle 1 to cycle 3 for native tissues, immersed and sonicated scaffolds increased from 13.69±0.99 to 17.21±0.98, 15.23±0.37 to 20.70±1.08 and 14.42±0.48 to 19.75±1.20, respectively. Stiffness and compression data for immersed and sonicated scaffolds were higher compared to native tissues, but there was a significant difference in compression data from cycle 2 and cycle 3 for immersion scaffold when compared with native tissues. In contradiction, the residual force data for native tissues were higher than both decellularized scaffolds with a significant difference for immersion treatment in cycle 1 and cycle 2.

Discussion

The healing potential of the meniscus tissues remains low due to limited vascular penetration in only one-third of tissues. Throughout the years, multiple clinical strategies had been conducted to develop a substitute as a replacement for the damaged tissues. One of the latest approaches is through the promising tissue engineering and regenerative medicine which aims to prepare a meniscus allograft or xenograft scaffolds for new tissue regeneration. These

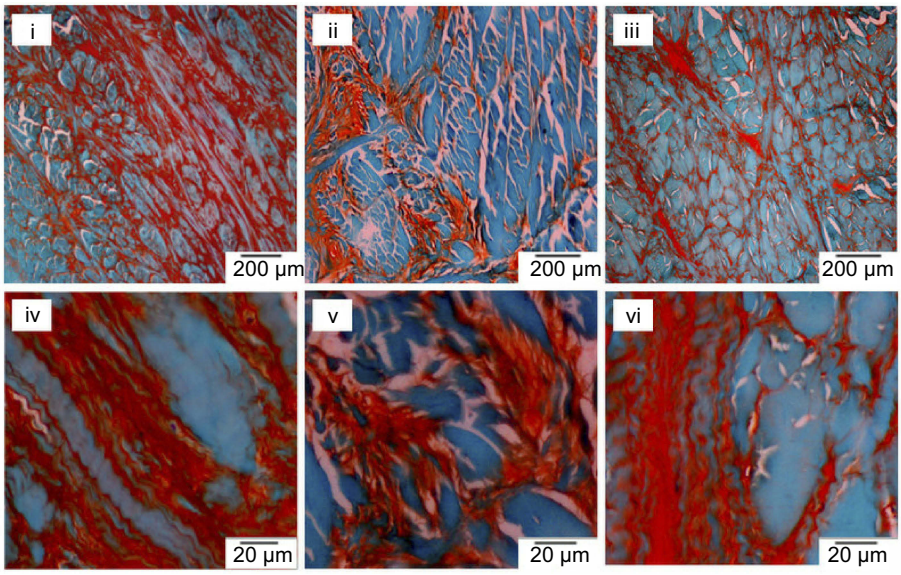

Figure 6 Safranin O/fast green staining of native (i, iv), immersed scaffolds (ii, v) and sonicated scaffolds (iii, vi) with a magnification of 4× (i, ii, iii) and 40× (iv,v,vi).

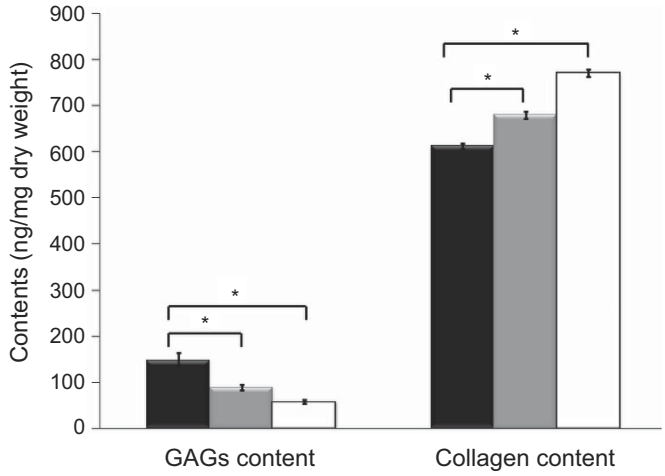

Figure 7 Collagen and GAG content in native (black), immersed (grey) and sonicated meniscus scaffolds (white). Significant difference: *p*-value<0.05.
Abbreviation: GAG, glycosaminoglycan

biological scaffolds are prepared through various decellularization processes which remove all of the cellular components while retaining the ECMs and biomechanical strength. Numerous decellularization procedures that comprised of chemical, biological and physical agents are available and studied up until now.[18,19] Thus, a proper procedure is required to prepare an ideal biological scaffold which is biocompatible, biodegradable and mechanically stable and have an optimal scaffold architecture.[20]

In our research, the ultimate goal is to prepare a meniscus bioscaffold with retained ECMs and biomechanical strength using sonication treatment system with 40 kHz frequency and 0.1% SDS solution. Three acceptance criteria of an effective decellularization have been described previously by Crapo et al which must be achieved to reduce the potential immunological response of the host toward the constructs. First and foremost, there should be no signs of nuclei stained through histology staining, low amount of residual DNA content and <200 bp DNA fragments obtained through gel electrophoresis analysis.[18]

Based on the results, it indicated that the sonicated scaffolds had no nuclei stained with low DNA content which were observed through H&E staining and residual DNA quantification. It was analyzed that there was a decrease of almost 92% of residual DNA content in

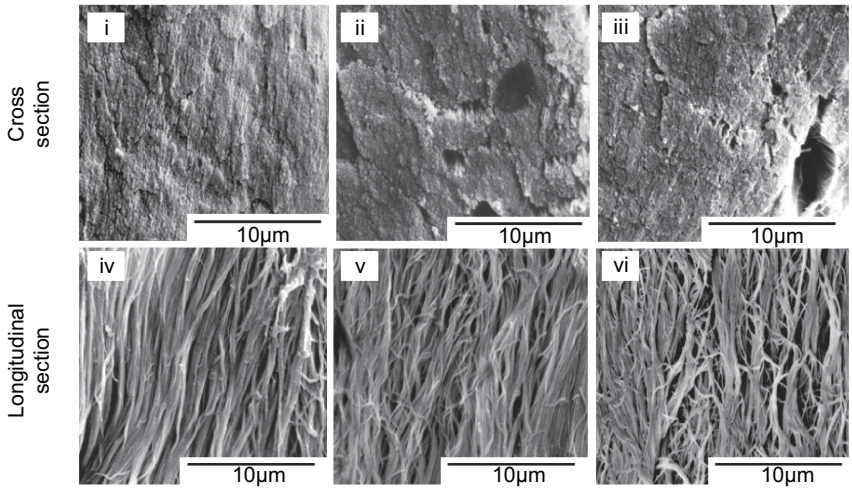

Figure 8 Surface ultrastructure from longitudinal and cross-section of native (i, iv), immersed (ii, v) and sonicated (iii, vi) scaffolds with 5,000x magnification.

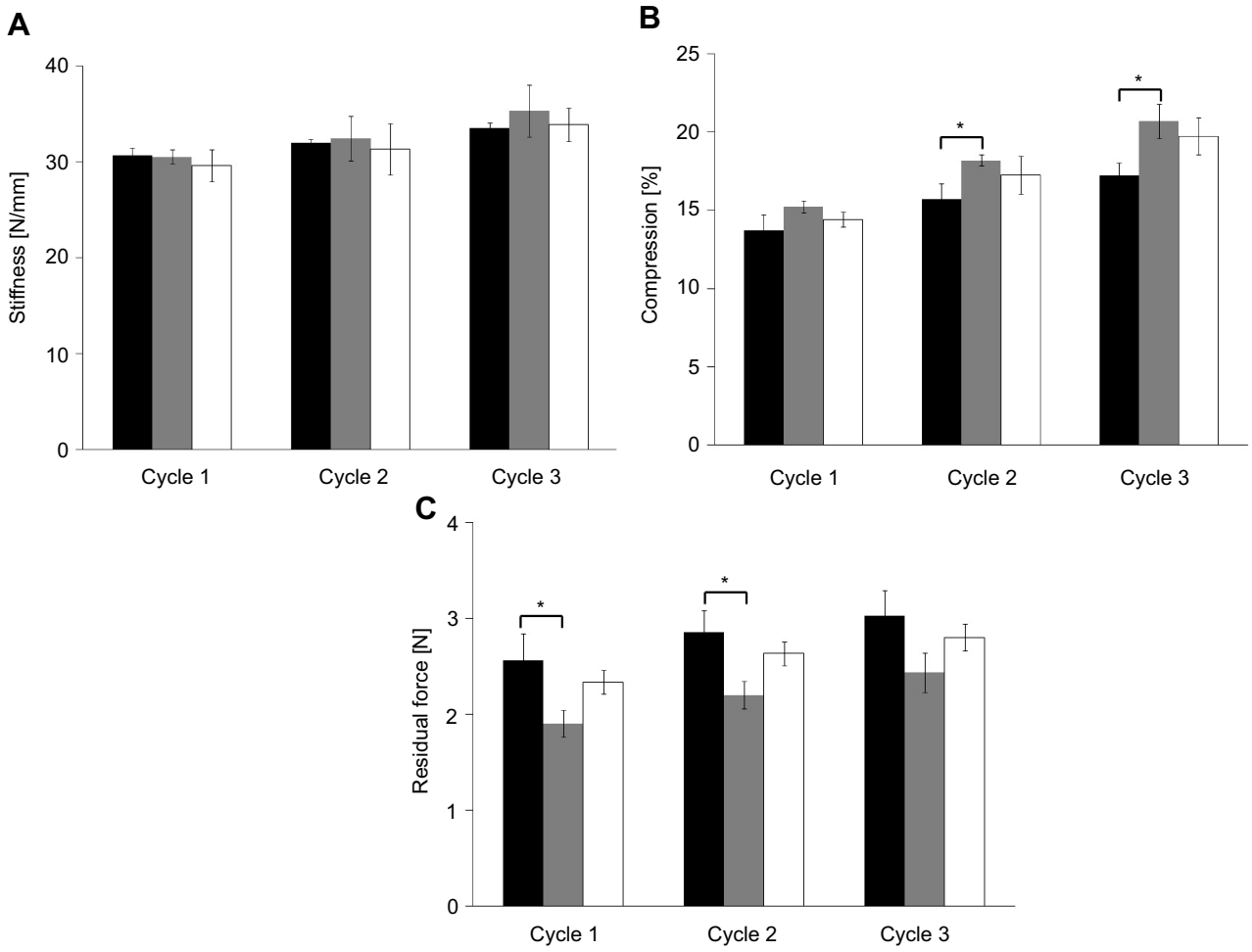

Figure 9 Bar graphs of biomechanical properties comprised of stiffness, compression and residual force for native (black), immersed (grey) and sonicated scaffolds (white). Significant difference: *p<0.05.

sonicated scaffolds compared to 68% in immersed scaffolds. However, the rate of DNA removal can be improved by increasing the treatment time and sonication intensity. Based on a previous study, it was reported that sonication intensity has a high correlation with decellularization rate.[21]

Decellularization using immersion treatment was found to be insufficient to achieve complete cell removal compared to the sonication treatment system. This was because SDS is the only chief agent for decellularization. As for sonicated scaffolds, the decellularization was completed by application of 40 kHz frequency and SDS detergent. SDS is an anionic surfactant which was classified as a harsh chemical and it was reported as one of the effective chemicals for decellularization process.[2,22] The SDS detergent triggered cell lysis process through the formation of micelles that solubilized the cell membrane, nuclear membrane and hydrophobic proteins.[23–25]

Sonication mechanism itself contributed to the decellularization process with two assumptions has been made. First and foremost, it was suspected that the application of 40 kHz sonication emitted the vibration in the aqueous SDS solution, which subsequently eases and assists the infiltration of SDS thoroughly from the surface cells to the interior cells. Second, the generation of acoustic cavitation bubbles occurred that expand in size and burst which induced shear stress effect, thus disrupting the integrity of cellular membrane lining.[13–16,21,26,27]

The application of the ultrasound to the liquid medium generates waves created by mechanical vibration comprised of rarefaction and compression phase.[26] The oscillations of the bubbles with positive and negative pressure will create acoustic cavitations with short lifetime. According to previous studies, there were two types of cavitations, namely, stable and unstable (inertial) cavitations.[28–33] For stable cavitations, the microbubbles have a balance oscillation process which maintains the size of bubble without undergoing violent collapse.[29,30] Different from inertial cavitations, the bubbles grow in successive cycles and experienced an expansion of the initial size of bubbles until an unstable size is reached followed by violent collapse with localized extreme temperature and pressure generated through microjet.[31] The remaining small fractions of the collapsed bubbles may rebound to grow and re-expand again to repeat the same process.[31,34]

Following the extreme collapse of bubbles, two sorts of physical and chemical effects are generated in the respective area of the event. For physical effect, the collapsed cavitation bubbles caused intense shock waves emitted in the surrounding liquid medium and causing shear stress on the membrane of the tissues. The shear stress acting on the tissue surface causes membrane disruption process which results in membrane integrity alteration, membrane invagination, pore formation and cell lysis.[33–37] As a consequence of this occurrence, it enhances membrane permeability and assists the SDS to infiltrate throughout tissue structure more rapidly.

In chemical effect, the extreme conditions of the collapsed bubbles caused pyrolyis of water and surfactant molecules which form the free radicals $OH\cdot$, $H\cdot$, $O2\cdot$ superoxide and surfactant derived radicals ($R\cdot$), respectively.[33,38] Normally, the free radicals $OH\cdot$ recombine with $H\cdot$ to form water molecules. However, the presence of surfactant radicals tends to compete for a reaction to produce secondary organic radicals known as alkylperoxyl radicals. These radicals are reported to have a relatively long lifetime, and once it reaches the cell membrane, the radicals tend to initiate chain reactions important for cell damage process.[39]

Considerable challenges need to be encountered for the decellularization process to have an optimum balance between the cell removal and retention of vital bioactive molecules within the scaffolds. Our developed sonication treatment system has portrayed the preservation of collagen and GAGs within the scaffolds. Collagen is the main fibrillar component within meniscus which has different collagen types based on the region of the tissue.[40,41] The collagen network distribution of the scaffolds was distinguished by picro-sirius red staining under polarized light and quantitatively using collagen content assay. Sonicated scaffolds demonstrated preserved intact collagen networks compared to porous networks obtained from immersed scaffolds. The diffusion limitation present in the immersion treatment was the chief cause of porous collagen networks in the scaffolds. The principle of SDS infiltration into the compact tissue structure of meniscus during immersion treatment was through slow simple diffusion. This leads the SDS to lyse the cells at the surface of tissue first followed by the interior cells. However, the initial lysis of surface cells caused the release of protease enzymes that are able to destroy the proteins within the extracellular matrix of the tissues which might be the reason for porous collagen network distribution.[42,43] Different from sonicated scaffolds, the 40 kHz frequency facilitated the superior infiltration of SDS agent that caused the cells at the surface and interior of tissue to lyse simultaneously. Consequently, lack protease enzyme was produced, and thus prevented the disruption of collagen fibrils. ti.

Biochemical assays for collagen content quantification further verified the retention of collagen networks within the scaffolds. Referring to Figure 7, decellularized scaffolds

had a significant increase in collagen content compared to native tissues, which were consistent with the previously reported study.[44] Decellularization process resulted in higher fractions of collagen per dry weight compared to native tissues due to the relevant removal of cellular, GAGs and other components during the decellularization process.[45–47] The result pattern obtained was consistent with a study done by Wu et al which utilized 1% SDS detergent to decellularize meniscus. The study found that due to the non-water soluble characteristics of the collagen fibers, the decellularization agent does not interfere with or damage the collagen network distribution and content.[44] Based on the combined results from picro-sirius red staining and collagen quantification, it was expected that the distribution and content of collagen networks within sonicated scaffolds were well retained and preserved.

The preservation of ECM compositions within the scaffolds was further confirmed by surface ultrastructure examination. This surface ultrastructure of sonicated scaffolds showed preserved collagen fibrils orientation and arrangement that resembles native tissues but had minor disruption with empty micropore structure which believed to represent the cells lacunae. As for immersion treatment, the process with poor agitation had caused an uneven decellularization process to remove the cells within the tissue structure. This was due to limited diffusion rate. In consequence, the prepared immersed scaffolds tend to possess an asperity-like structure with the appearance of cavities.

Proteoglycans consist of a core protein decorated by various types of GAGs which covered 15% of the organic matter in meniscus tissues.[1,41] The negatively charged GAGs perform important roles in maintaining the tissue hydration and compressive stiffness by attracting water molecules within the matrix.[1] Based on safranin O/fast green staining, sonicated scaffolds had deficient GAGs stained compared to native but managed to preserve the distribution. Additionally, there was a significant reduction of GAG content in immersed and sonicated scaffolds. GAGs are known as water-soluble components. The result was consistent with the previous study done by Stapleton that used SDS as the decellularizing agent.[48] As the decellularization was conducted in SDS solution, it is likely that this detergent separates the GAGs by disrupting the links with the core proteins.[31] Further loss of water-soluble GAGs occurred due to the process conducted in an aqueous solution which can easily wash away the separated GAGs from the tissues.[44] According to Hrebíková, the chemical detergent SDS has a deleterious effect on the GAG content within the tissues.[49] From the previous study, it revealed that GAG reduction after the decellularization process is a crucial step for future in vitro study. Subsequently, it will contribute to increase the tissue structure porosity and enable migration of the cells into the scaffolds.[50]

The biomechanical properties of the prepared meniscus scaffolds are essential to be preserved as meniscus has an important role in load transmission and as a shock absorber.[1] The biomechanical strength of this fibrocartilaginous tissue was reported to derive from the ECMs.[51] Responte revealed that the integrity of the tissues is contributed by collagen, while GAGs are responsible for the compressive strength.[52] For residual forces, the decellularized scaffolds had lower values compared to native tissues which illustrated a decrease in elastic properties. A high residual force within the tissue will have more elastic than viscous and vice versa. This circumstance was due to the decellularization treatment which caused the structural changes within the ECM including the partial GAGs removal and formation of micropores with loose collagen fibril tension. Based on biochemical assays, the GAG which is crucial in maintaining the water content was partially removed in decellularized scaffolds. The depletion of GAGs within decellularized scaffolds had led to low residual forces obtained. However, it negatively affects the biomechanical properties as there was no significant difference discovered between native and decellularized scaffolds.

Based on compression data, the sonicated scaffolds had a higher percentage compared to native tissue without significant difference. This result demonstrated that the viscosity and elasticity of the sonicated scaffolds were notably high. Collagen network is the main constituent of ECM responsible for the tensile strength of meniscus tissues.[53] The circumferential collagen fibers in sonicated scaffolds were retained based on staining and biochemical assays after treatment which consequently maintains the stiffness of tissues. The factors that led to the increment of cyclic loading from cycle 1 to cycle 3 for all tissue samples for stiffness and residual forces were believed to be due to the gradual compression on the tissues that have a dense extracellular matrix.[54,55] Our results showed that the biomechanical properties with a statistically insignificant difference were not adversely influenced after the decellularization treatment using SDS with sonication frequency compared to SDS alone. This is because the inclusion of 40 kHz frequency enhances superior decellularization process and caused minor disruption of ECM compared to immersion treatment.

Conclusion

In conclusion, the decellularization of meniscus tissues derived from bovine was successfully completed using the developed sonication treatment system. The H&E staining and DNA quantification portrayed that the syste abolished most of the cells from tissues. Besides, the prepared scaffolds managed to retain the matrix and biomechanical properties based on biomechanical strength characterization, biochemical assays for collagen and GAG content. Last, surface ultrastructure of the collagen fibrils within the sonicated tissues resembled native tissues with minor disruption on the orientation. Therefore, sonication treatment system would be a promising decellularization technique for orthopedic tissue engineering applications. Further study for in vitro and in vivo are needed to examine the cytotoxicity and biocompatibility of the prepared scaffolds.

Acknowledgments

The authors are grateful to the Ministry of Higher Education for financial support through the Fundamental Research Grant Scheme (FRGS/1/2017/STG05/UIAM/02/6), the Prototype Research Grant Scheme (PRGS16-002-0033), and the Transdisciplinary Research Grant Scheme (TRGS16-02-001-0001).

Disclosure

The authors report no conflicts of interest in this work.

References

1. Fox AJ, Bedi A, Rodeo SA. The basic science of human knee menisci. *J Sports Health*. 2012;4(4):340–351. doi:10.1177/1941738111429419
2. Gao S, Yuan Z, Xi T, Wei X, Guo Q. Characterization of decellularized scaffold derived from porcine meniscus for tissue engineering applications. *Front Mater Sci*. 2016;10(2):101–112. doi:10.1007/s11706-016-0335-y
3. Howell RL, Kumar NS, Patel NM, Tom J. Degenerative meniscus: pathogenesis, diagnosis, and treatment options. *World J Orthop*. 2014;5(5):597–602. doi:10.5312/wjo.v5.i5.597
4. Greis PE, Bardana DD, Holmstrom MC, Burks RT. Meniscal injury: I. Basic science and evaluation. *J Am Acad Orthopedic Surgeons*. 2002;10(3):168–176. doi:10.5435/00124635-200205000-00003
5. Makris EA, Hadidi P, Athanasiou KA. The knee meniscus: structure-function, pathophysiology, current repair techniques, and prospects for regeneration. *Biomaterials*. 2011;32(30):7411–7431. doi:10.1016/j.biomaterials.2011.06.037
6. Jeong HJ, Lee SH, Ko CS. Meniscectomy. *Knee Surg Relat Res*. 2012;24(3):129–136. doi:10.5792/ksrr.2012.24.3.129
7. Doral MN, Bilge O, Huri G, Turhan E, Verdonk R. Modern treatment of meniscal tears. *EFORT Open Rev*. 2018;3(5):260–268. doi:10.1302/2058-5241.3.170067
8. Brindle T, Nyland J, Johnson DL. The meniscus: review of basic principles with application to surgery and rehabilitation. *J Athl Train*. 2001;36(2):160–169.
9. Smith NA, Costa ML, Spaldin T. Meniscal allograft transplantation: rationale for treatment. *Bone Joint J*. 2015;97-B(5):590–594. doi:10.1302/0301-620X.97B5.35152
10. Tucker B, Khan W, Al-Rashid M, Al-Khateeb H. Tissue engineering for the Meniscus: a review of the literature. *Open Orthopedics J*. 2012;6:348–351. doi:10.2174/1874325001206010348
11. Keane TJ, Swinehart I, Badylak SF. Methods of tissue decellularization used for preparation of biologic scaffolds and in vivo relevance. *Methods*. 2015;84:25–34. doi:10.1016/j.ymeth.2015.03.005
12. Gilbert TW. Strategies for tissue and organ decellularization. *J Cell Biochem*. 2012;113(7):2217–2222. doi:10.1002/jcb.24130
13. Azhim A, Yamagami K, Muramatsu K, Morimoto Y, Tanaka M. The use of sonication treatment to completely decellularize blood arteries: a pilot study. *Conf Proc IEEE EMBS*. 2011;2011: 2468–2471.
14. Azhim A, Syazwani N, Morimoto Y, Furukawa K, Ushida T. The use of sonication treatment to decellularize aortic tissues for preparation of bioscaffolds. *J Biomater Appl*. 2014;29(1):130–141. doi:10.1177/0885328213517579
15. Syazwani N, Azhim A, Marimoto Y, Furukawa K, Ushida T. Immune response of implanted aortic as scaffolds decellularized by sonication treatment. *IFMBE Proceedings*. 2014;43:275-278.
16. Syazwani N, Shafiq M, Ushida T, Azhim A. Simulation and Experimental Measurement of Acoustic Intensity on Sonication Parameters and Decellularization using Sonication Treatment. *Journal of Signal Processing*. 2015;19(4):179-182.
17. Azhim A, Takahashi T, Muramatsu K, Morimoto Y, Tanaka M. Decellularization of meniscal tissue using ultrasound chemical process for tissue-engineered scaffold applications. *IFMBE Proc*. 2010;31:915–918.
18. Crapo PM, Gilbert TW, Badylak SF. An overview of tissue and whole organ decellularization processes. *Biomaterials*. 2011;32(12):3233–3243. doi:10.1016/j.biomaterials.2011.01.057
19. Gupta SK, Mishra NC, Dhasmana A. Decellularization methods for scaffold fabrication. In: Turksen K, editor. *Decellularized Scaffolds and Organogenesis. Methods in Molecular Biology*. Vol. 1577. New York, NY: Humana Press; 2017:1–10.
20. O'Brien FJ. Biomaterials and scaffolds for tissue engineering. *Mate Today*. 2011;14(3):88–95. doi:10.1016/S1369-7021(11)70058-X
21. Azhim A, Shafiq M, Rasyada A, Furukawa K, Ushida T. The impact of acoustic intensity on solution parameters and decellularization using sonication treatment. *J Biomater Tissue Eng*. 2015;5(3):195–203. doi:10.1166/jbt.2015.1300
22. Gilpin A, Yang YG. Decellularization strategies for regenerative medicine: from processing techniques to applications. *Biomed Res Int*. 2017. doi:10.1155/2017/9831534
23. Faulk DM, Carruthers CA, Warner HJ, et al. The effect of detergents on the basement membrane complex of a biologic scaffold material. *Acta Biomater*. 2014;10(1):183–193. doi:10.1016/j.actbio.2013.09.006
24. White LJ, Taylor AJ, Faulk DM, et al. The impact of detergents on the tissue decellularization process: a ToF-SIMS study. *Acta Biomater*. 2017;50:207–219. doi:10.1016/j.actbio.2016.12.033
25. Keane TJ, Swinehart IT, Badylak SF. Methods of tissue decellularization used for preparation of biologic scaffolds and in vivo relevance. *Methods*. 2015;84:25–34. doi:10.1016/j.ymeth.2015.03.005
26. Azhim A, Yamagami K, Muramatsu K, et al. The use of sonication treatment to completely decellularize aorta tissue. *IFMBE Proc*. 2013;39:1987–1990.
27. Syazwani N, Azhim A, Morimoto Y, Furukawa K, Ushida T. Decellularization of aorta tissue using sonication treatment as potential scaffold for vascular tissue engineering. *J Med Biol Eng*. 2015;35(2):258–269. doi:10.1007/s40846-015-0028-5
28. Wu TY, Guo N, Teh CY, Hay JXW. Theory and Fundamentals of Ultrasound. In: *Advances in Ultrasound Technology for Environmental Remediation*. New York: Springer Netherlands; 2013:5–12.

29. Peruzzi G, Sinibaldi G, Silvani G, Ruocco G, Casciola CM. Perspectives on cavitation enhanced endothelial layer permeability. *Colloids Surf B*. 2018;168:83–93. doi:10.1016/j.colsurfb.2018.02.027
30. Jiménez-Fernández J, Crespo A. Bubble oscillation and inertial cavitation in viscoelastic fluids. *Ultrasonics*. 2005;43(8):643–651. doi:10.1016/j.ultras.2005.03.010
31. Dawson P. The physics of the oscillating bubble made simple. *Eur J Radiol*. 2002;41(3):176–178.
32. Mason TJ, Joyce E, Phull SS, Lorimer JP. Potential uses of ultrasound in the biological decontamination of water. *Ultrason Sonochem*. 2003;10:319–323. doi:10.1016/S1350-4177(03)00102-0
33. Mullick A, Neogi S. A review on acoustic methods of algal growth control by ultrasonication through existing and novel emerging technologies. *Rev Chem Eng*. 2016;33(5):1–23.
34. Miyoshi N, Sostaric JZ, Riesz P. Correlation between sonochemistry of surfactant solutions and human leukemia cell killing by ultrasound and porphyrins. *Free Radic Biol Med*. 2003;34(6):710–719. doi:10.1016/S0891-5849(02)01428-4
35. Gogate PR, Kabadi AM. A review of applications of cavitation in biochemical engineering/biotechnology. *Biochem Eng J*. 2009;44(1):60–72. doi:10.1016/j.bej.2008.10.006
36. Juffermans LJ, Dijkmans PA, Musters RJ, Visser CA, Kamp O. Transient permeabilization of cell membranes by ultrasound-exposed microbubbles is related to formation of hydrogen peroxide. *Am J Physiol Heart Circulatory Physiol*. 2006;291(4):H1595–H1601. doi:10.1152/ajpheart.01120.2005
37. Schlicher RK, Radhakrishna H, Tolentino TP, Apkarian RP, Zarnitsyn V, Prausnitz MR. Mechanism of intracellular delivery by acoustic cavitation. *Ultrasound Med Biol*. 2006;32(6):915–924. doi:10.1016/j.ultrasmedbio.2006.02.1416
38. Juffermans LJ, van Dijk A, Jongenelen CA, et al. Ultrasound and microbubble-induced intra-and intercellular bioeffects in primary endothelial cells. *Ultrasound Med Biol*. 2009;35(11):1917–1927. doi:10.1016/j.ultrasmedbio.2009.06.1091
39. Alfassi ZB, Huie RE, Neta P. Kinetic studies of organic peroxyl radicals in aqueous solutions and mixed solvents. In: Alfassi ZB, editor. *Peroxyl Radicals*. West Sussex, UK: John Wiley and Sons Ltd.; 1997:235–281.
40. Athanasiou KA, Adams JS. *Engineering the Knee Meniscus.* San Rafael:Morgan & Claypool Publishers; 2009:1–83.
41. Pereira H, Silva-Correia J, Oliveira JM, Reis RL, Espregueira-Mendes J. The meniscus: basic science. In: Verdonk R, Espregueira Mendes J, Monllau J, editors. *Meniscal Transplantation*. Berlin, Heidelberg: Springer; 2013:7–14.
42. Seetapun D, Jeffrey JR. Eliminating the organ transplant waiting list: the future with perfusion decellularized organs. *Surgery*. 2017;161(6):1474–1478. doi:10.1016/j.surg.2016.09.041
43. Eleta G, Roger O, Cartoline T, et al. Tissue engineering by decellularization and 3D bioprinting. *Mate Today*. 2017;20(4):166–178. doi:10.1016/j.mattod.2016.12.005
44. Wu J, Ding Q, Dutta A, et al. An injectable extracellular matrix derived hydrogel for meniscus repair and regeneration. *Acta Biomater*. 2015;16:49–59. doi:10.1016/j.actbio.2015.01.027
45. Baptista PV, Siddiqui MM, Lozier G, Rodriguez SR, Atala AJ, Soker S. The use of whole organ decellularization for the generation of a vascularized liver organoid. *Hepatology*. 2011;53(2):604–617. doi:10.1002/hep.24067
46. Sabetkish S, Kajbafzadeh A, Sabetkish N, et al. Whole-organ tissue engineering: decellularization and recellularization of three-dimensional matrix liver scaffolds. *J Biomed Mater Res Part A*. 2015;103(4):1498–1508. doi:10.1002/jbm.a.35291
47. Struecker B, Hillebrandt KH, Voitl R, et al. Porcine liver decellularization under oscillating pressure conditions: a technical refinement to improve the homogeneity of the decellularization process. *Tissue Eng Part C Methods*. 2015;21(3):303–313. doi:10.1089/ten.TEC.2014.0321
48. Stapleton TW, Ingram JH, Katta J, et al. Development and characterization of an acellular porcine medial meniscus for use in tissue engineering. *Tissue Eng Part A*. 2008;14(4):505–518. doi:10.1089/tea.2007.0233
49. Hrebíková H, Diaz DS, Mokry J. Chemical decellularization: a promising approach for preparation of extracellular matrix. *Biomedical Papers*. 2015;159(1):12–17. doi:10.5507/bp.2013.076
50. Schwarz S, Koerber L, Elsaesser AF, et al. Decellularized cartilage matrix as a novel biomatrix for cartilage tissue-engineering applications. *Tissue Eng Part A*. 2012;18(21–22):2195–2209. doi:10.1089/ten.TEA.2011.0705
51. Eleswarapu SV, Responte DJ, Athanasiou KA. Tensile properties, collagen content, and crosslinks in connective tissues of the immature knee joint. *PLoS One*. 2011;6(10):1–7. doi:10.1371/journal.pone.0026178
52. Responte DJ, Natoli RM, Athanasiou KA. Collagens of articular cartilage: structure, function, and importance in tissue engineering. *Crit Rev Biomed Eng*. 2007;35:363–411. doi:10.1615/CritRevBiomedEng.v35.i5.20
53. Herwig J, Egner E, Buddecke E. Chemical changes of human knee joint menisci in various stages of degeneration. *Ann Rheum Dis*. 1984;43:635–640. doi:10.1136/ard.43.4.635
54. Sandmann GH, Eichhorn S, Vogt S, et al. Generation and characterization of a human acellular meniscus scaffold for tissue engineering. *J Biomed Mater Res Part A*. 2008; 91A(2):567–574.
55. Maier D, Braeun K, Steinhauser E, et al. In vitro analysis of an allogenic scaffold for tissue-engineered meniscus replacement. *J Orthopedic Res*. 2007;25(12):1598-1608.